

Scientific paper

# Toluene, Methanol and Benzaldehyde Removal from Gas Streams by Adsorption onto Natural Clay and Faujasite-Y type Zeolite

Hicham Zaitan,<sup>1,\*</sup> Elham F. Mohamed,<sup>2</sup> Héctor Valdés,<sup>3</sup> Mostafa Nawdali,<sup>4</sup> Salah Rafqah<sup>5</sup> and Marie Hélène Manero<sup>6</sup>

<sup>1</sup> Laboratoire de Chimie de la Matière Condensée, Faculté des Sciences et Techniques, Université Sidi Mohamed Ben Abdellah, Fès, Maroc.

<sup>2</sup> Air Pollution Department, Environmental Research Division, National Research Centre, 33 EL Bohouth St., Dokki, Giza, Egypt.

<sup>3</sup> Laboratorio de Tecnologías Limpías (F. Ingeniería), Universidad Católica de la Santísima Concepción, Alonso de Ribera 2850, Concepción, Chile

<sup>4</sup> Laboratoire de Chimie de la Matière Condensée, Faculté Polydisciplinaire de Taza, Université Sidi Mohamed Ben Abdellah, Taza, Maroc

<sup>5</sup> Laboratoire de Chimie Analytique et Moléculaire, Faculté Polydisciplinaire, Safi, Université Cadi Ayyad, Marrakech, Maroc.

<sup>6</sup> Université de Toulouse, INPT, UPS, Laboratoire de Génie Chimique, 4, Allée Emile Monso, F-31030 Toulouse, France

\* Corresponding author: E-mail: [hicham.zaitan@usmba.ac.ma](mailto:hicham.zaitan@usmba.ac.ma) (Hicham Zaitan)  
Tel: +212- 535611686; Fax.: +212- 535608214

Received: 01-06-2016

## Abstract

A great number of pollution problems come as a result of the emission of Volatile Organic Compounds (VOCs) into the environment and their control becomes a serious challenge for the global chemical industry. Adsorption is a widely used technique for the removal of VOCs due to its high efficiency, low cost, and convenient operation. In this study, the feasibility to use a locally available clay, as adsorbent material to control VOCs emissions is evaluated. Natural clay is characterised by different physical-chemical methods and adsorptive interaction features between VOCs and natural clay are identified. Toluene (T), methanol (M) and benzaldehyde (B) are used here as representatives of three different kinds of VOCs. Adsorption isotherms onto natural clay and faujasite-Y type zeolite (Fau Y) are obtained at room temperature. According to Langmuir model data, maximum adsorption capacities ( $q_m$ ) of Fez natural clay and zeolite toward methanol (M), toluene (T) and benzaldehyde (B) at 300 K are 8, 0.89 and 3.1 mmol g<sup>-1</sup>, and 15, 1.91 and 13.9 mmol g<sup>-1</sup> respectively. In addition, the effect of temperature on the adsorption of toluene onto natural clay is evaluated in the range from 300 to 323 K. An increase on temperature reduces the adsorption capacity of natural clay toward toluene, indicating that an exothermic physical adsorption process takes place. The enthalpy of adsorption of toluene onto Fez natural clay was found to be -54 kJ mol<sup>-1</sup>. A preliminary cost analysis shows that natural clay could be used as an alternative low cost adsorbent in the control of VOCs from contaminated gas streams with a cost of US\$ 0.02 kg<sup>-1</sup> compared to Fau Y zeolite with US\$ 10 kg<sup>-1</sup>.

**Keywords:** Adsorption, Air pollution control, Zeolite, Natural clay, VOCs.

## 1. Introduction

Various industrial processes are the main sources of volatile organic compounds (VOCs) that contribute to air

pollution issues.<sup>1–3</sup> VOCs are critical toxic substances that may cause harmful effects on human health when are emitted into the environment.<sup>4</sup> Additionally, they have ad-

verse environmental effects on vegetation and various kinds of materials.<sup>5</sup> Toluene, methanol, xylene, acetaldehyde and benzaldehyde are the most commonly used aromatic solvents in a great variety of industrial applications.

In USA, approximately  $12.3 \times 10^3$  kilotons of VOCs are released into the atmosphere from industrials and humans sources.<sup>6</sup> It is noted that 40% of the VOCs emissions are released from transportation activities and the remaining 60% results from stationary sources; being equally divided between fuel combustion, industrial manufacturing and solvent emissions. However, in case of Europe, the total VOC emissions are about  $9.4 \times 10^9$  kilotons in 2006.<sup>7</sup> VOC emissions are decreased by 44% in Europe since 1990. The European Commission sets an emission limit value (ELV) of 20 mg of VOCs/Nm<sup>3</sup> in a stream discharged into the atmosphere.<sup>8</sup>

The reduction of VOCs from gas waste streams to acceptable levels is a serious challenge for the global chemical industry. There are several available techniques for VOCs control.<sup>9–14</sup> Adsorption is the most preferred method for the removal of VOCs from polluted air. Moreover, adsorption is a very effective treatment method to use at low concentration levels of VOCs.<sup>15–16</sup> Activated carbons and zeolites have been widely used as adsorbents in many environmental applications.<sup>17–23</sup> On one hand, the use of activated carbons as adsorbents is limited by their high costs of manufacturing, pore blocking, flammability risk and other problems associated to their regeneration.<sup>24</sup> On the other hand, synthetic zeolites are regarded as effective but expensive adsorbents (10 times more than activated carbons) and in some cases sensitive to the presence of humidity.<sup>25</sup> In this perspective, different alternative adsorbents are desirable to overcome these kinds of problems.<sup>26–28</sup> In this context, natural clays appear as interest natural adsorbents to clean polluted air, since their application could result in a cost-effective process for VOCs removal. Natural clays are quite abundant and their low costs are likely to become strong adsorbent candidates for

the removal of VOCs from air. However, most of the studies of the use of natural clays are devoted to the adsorption of heavy metals or organic molecules from wastewater.<sup>29–30</sup> Very few studies are focused on the removal of VOCs from waste gaseous streams.<sup>31–35</sup>

The study presented here aims to evaluate the feasibility to use locally available clay normally used in the ceramic industry, as adsorptive material for the elimination of VOCs from waste gaseous streams. In particular, clay adsorption capacity toward different target VOCs are evaluated. Additionally, adsorption capacity of natural clay is compared to a commercial zeolite (Faujasite Y). Moreover, the influence of surface properties such as surface area and porosity on the adsorption capacity is discussed.

## 2. Material and Methods

### 2.1. Materials

Natural clay was obtained from deposits located in the vicinity of Fez city, Morocco (denoted here as FS) and was used without any previous activation. It was sieved into a range of 0.08–0.5 mm and washed with deionised water and then dried in air at 383 K for 24 h and stored in a dessicator until further use. A commercial dealuminated faujasite Y zeolite (Fau Y) was supplied by TOSOH Corporation (360HUD3C) (Tokyo, Japan) in the form of pellets (5 mm length  $\times$  3 mm diameter). Natural clay and Fau Y zeolite were dried in air at 383 K for 24 h and stored in a dessicator until further use. Physical and chemical surface properties of natural clay and Fau Y zeolite are listed in Table 1.

Methanol (M), benzaldehyde (B) and toluene (T) are used in this study as target VOCs, representatives of families of alcohols, aldehydes and aromatic organic compounds, respectively. They were supplied in liquid phase by Sigma-Aldrich (Sigma-Aldrich Chimie S.a.r.l., Lyon, France), all of them with a purity > 99%.

**Table 1.** Physical–chemical properties of FS natural clay and Fau Y zeolite

Property	FS natural clay	Faujasite Y zeolite
Origin	Fez area (Morocco)	Tosoh Corp. 360HUD3C (Japan)
Geometry	Granule (D = 0.08–0.5 mm)	Pellet (L = 5 mm, D = 3mm)*
Crystalline framework	–	$\alpha$ -cages
Pore diameters (Å)	8	7.4 (aperture) – 13 (cage Ø)
SiO <sub>2</sub> /Al <sub>2</sub> O <sub>3</sub> (mol mol <sup>-1</sup> )	5.71	13.7
Clay binder content (m %)	–	25%
Total pore volume V <sub>T</sub> (cm <sup>3</sup> g <sup>-1</sup> )	0.03	0.4
Specific surface area S <sub>BET</sub> (m <sup>2</sup> g <sup>-1</sup> )	29	550
Apparent density (g dm <sup>-3</sup> )	700	460
Material colour	Grey	White
Dominant clay mineral	Kaolinite	–

\* D: diameter, L: length

## 2. 2. Characterisation of Clay Sample

The surface area and pore volume of the FS natural clay were measured by Micromeritics ASAP 2010 instrument using nitrogen adsorption at 77 K after out degassing the clay natural at 383K for 6 hours in a vacuum of  $<10^{-3}$  Pa to remove all physically adsorbed water molecules and small organic impurities. The percentages of sand, silt and clay in the FS clay sample were measured on bulk sediment, using a laser diffraction particle analyser. Samples were dispersed in 100 cm<sup>3</sup> of deionised water and disaggregated under stirring using ultrasonic waves output of 1000 kW, and a vibration giving time of 10 min.<sup>36</sup>

Mineralogical composition of natural clay was determined by powder X-ray diffraction analysis (XRD) using X'Pert PRO Philips diffractometer (Philips Japan, Ltd, Japan), equipped with CuK $\alpha$  radiation ( $\lambda = 1.5406$  Å) at 40 kV and 40 mA. Runs were carried out using a step width of  $0.03^\circ 2\theta$ , registering every 1 s per step over the range  $2 < \theta < 70^\circ$ . Different phases were identified using database of the International Centre for Diffraction Data (ICDD). Elemental composition of the clay sample was identified by X-ray fluorescence (XRF) using a Bruker S4 Pioneer spectrometer. Particle size distribution was determined using a laser diffraction particle analyser. Total organic matter content was quantified by measurements of loss on ignition. Atterberg limit of raw clay was also established.

Scanning electron microscopy assays (SEM) were conducted with a QUANTA-200 scanning electron microscope (Philips). Accelerating voltages were measured between 1 and 30 kV with increments of 1kV. Scanning electron microscope provides a surface image with a resolution of a few tens of nm. This technique gives information about solid surface morphology (size, shape and pore distribution).

Thermogravimetric analyses (TGA) were carried out in a thermobalance apparatus (Seteram TGA-92). FS natural clay sample (0.0165 g), was heated up to 1273 K (heating rate of 10 K min<sup>-1</sup>) under air flow (30 cm<sup>3</sup> min<sup>-1</sup>) and the change in sample weight in relation to change in temperature was registered (TG curve). FTIR spectra were measured by the VERTEX70 spectrometer in the range 4000 to 400 cm<sup>-1</sup> with a resolution of 4 cm<sup>-1</sup> in order to investigate the surface characteristics of FS natural clay.

## 2. 3. Adsorption Isotherms

VOCs adsorption isotherms were performed using the bottle point method, as described elsewhere.<sup>37</sup> Figure 1 shows a schematic representation of the experimental system used to determine the adsorption performance. Adsorbent samples (FS natural clay or Fau Y zeolite) were introduced into the angled tube (0.5 g) of the batch glass contactor (1.1 dm<sup>3</sup>). Then, a known volume of liquid VOC was injected through a septum into each adsorption chamber at 300 K and 101 kPa, leading to a desired initial VOC concentration after its complete evapo-

ration. The effect of temperature on adsorption of VOC was studied at three temperatures (300, 313 and 323K). Adsorption chambers were stirred until equilibrium was reached (ca. 2 h).

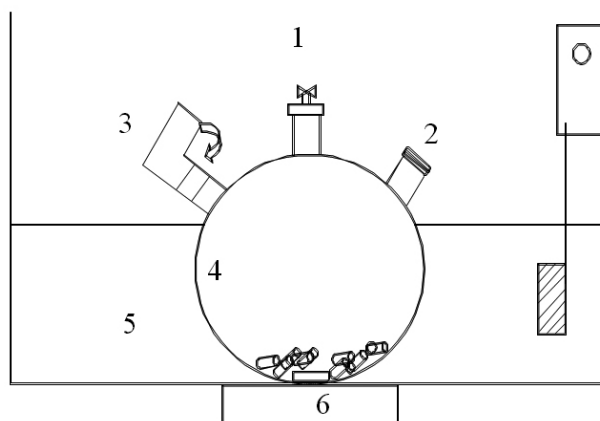


**Figure 1.** Experimental device for adsorption isotherm determination: (1) valve for gas sampling, (2) liquid injection septum, (3) angled tube containing the adsorbent, (4) bottle contactor, (5) thermostatic bath and (6) stirring system.

Finally, gas samples were taken from each bottle and analysed by gas chromatography (Varian CP-3800 GC, Varian Inc., USA). The total amount of adsorbed VOC per gram of adsorbent at equilibrium,  $q_e$  (mol kg<sup>-1</sup>), was calculated from a mass balance in each isotherm batch adsorption chamber, as follows:

$$q_e = V (C_0 - C_e)/m \quad (1)$$

where  $C_0$  and  $C_e$  (mol m<sup>-3</sup>) are gas phase concentration of the selected VOCs at the beginning and at equilibrium, respectively.  $m$  (g) is the mass of adsorbent sample used in each batch adsorption chamber, and  $V$  ( $1.1 \times 10^{-3}$  m<sup>3</sup>) stands for the total volume of the adsorption chamber.

## 3. Results and discussion

### 3. 1. Characterisation of Clay Sample

Fig. 2 and Table 2 summarise the textural properties of the sample measured by the physical adsorption of N<sub>2</sub> at 77K. The FS natural clay shown type IV isotherm according to the IUPAC classification. The initial part of the Type IV isotherm ( $P/P_0 < 0.4$ ), corresponding to the monolayer region, was scarcely visible, which could be ascribed to physical adsorption at the surface of the adsorbent. In a high relative pressure range, the isotherm show a clear hysteresis loop associated with capillary condensation taking place in mesopores structures,<sup>32</sup> formed between the elementary clay particles named tactoids.

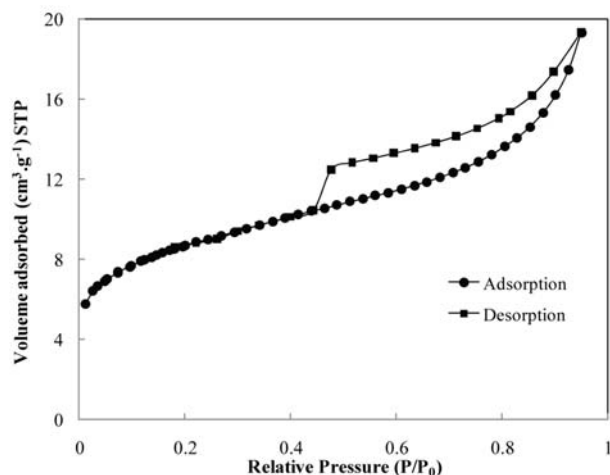


Figure 2. N<sub>2</sub> isotherm of FS clay

As shown in Table 2, BET surface area of the FS clay is 29 m<sup>2</sup>/g with an average pore diameter ranging from 2.1 nm.

Table 2: Textural parameters of FS natural clay

Parameter	Calculated value
$S_{\text{BET}}$ (m <sup>2</sup> g <sup>-1</sup> )	29
$V_t^a$ (cm <sup>3</sup> g <sup>-1</sup> )	0.030
$V_{\text{meso}}^b$ (cm <sup>3</sup> g <sup>-1</sup> )	0.025
$S_{\text{ext}}^c$ (m <sup>2</sup> g <sup>-1</sup> )	20
$S_{\text{mic}}^d$ (m <sup>2</sup> g <sup>-1</sup> )	9
$V_{\text{mic}}^e$ (cm <sup>3</sup> g <sup>-1</sup> )	0.005
$D_p^f$ (nm)	2.1

<sup>a</sup> Total pore volume, <sup>b</sup> Mesoporous volume, <sup>c</sup> External specific surface, <sup>d</sup> Specific micropore surface area, <sup>e</sup> Microporous volume, <sup>f</sup> pore diameter

Particle size distribution analysis shows that FS natural clay is a smooth solid material composed by 1 % of sand (>80 μm), 49% of silt (ranged 2–80 μm) and 50% of clay (< 2 μm). A high clay content is normally related to material plasticity; however organic matter content and other parameters are also involved. A more detailed evaluation of clay plasticity was conducted using the Atterberg Limits.<sup>38,39</sup> Results evidence a liquid limit (LL) of 56%, a plastic limit (PL) of 20%, and a plasticity index (PI) of 36%. Additionally, chemical analysis shows that FS contains 14.29 % of carbonates (expressed as CaCO<sub>3</sub>) and only a 3% of organic matter.

Fig. 3 shows the mineralogical composition of FS natural clay. Results reveal a complex heterogeneous structure of FS natural clay, corresponding to quartz (Q) and calcite (C). Semi-quantitative analyses indicate that natural clay is mainly composed by smectite (35%), kaoli-

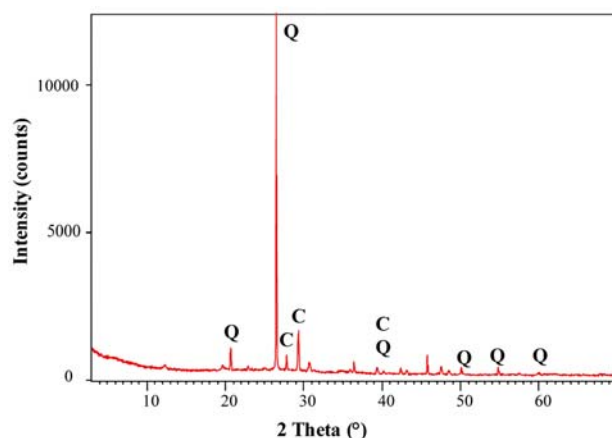


Figure 3. X-ray diffraction of FS natural clay (Q: Quartz, C: Calcite)

nite (25%), illite (20%), chlorite (10%) and inter-stratified minerals (10%).

XRF results (see Table 3) indicate that FS natural clay is mainly composed of SiO<sub>2</sub>, Al<sub>2</sub>O<sub>3</sub>, CaO, and Fe<sub>2</sub>O<sub>3</sub>; with a SiO<sub>2</sub>/Al<sub>2</sub>O<sub>3</sub> of 3.4 and trace amount of other oxides such as MgO, K<sub>2</sub>O, Na<sub>2</sub>O, P<sub>2</sub>O<sub>5</sub>, TiO<sub>2</sub>. Fau zeolite is composed of SiO<sub>2</sub> and Al<sub>2</sub>O<sub>3</sub> followed by K<sub>2</sub>O, Fe<sub>2</sub>O<sub>3</sub>, MgO and Na<sub>2</sub>O, with a SiO<sub>2</sub>/Al<sub>2</sub>O<sub>3</sub> of 1.8.

Table 3. Chemical composition of raw FS natural clay and Fau Y zeolite (m%) determined by XRF.

	FS natural clay	Fau Y
SiO <sub>2</sub>	41.28	28.0
Al <sub>2</sub> O <sub>3</sub>	12.29	16.0
Fe <sub>2</sub> O <sub>3</sub>	4.13	1.0
MgO	2.80	0.6
K <sub>2</sub> O	1.74	5.6
CaO	14.23	–
Na <sub>2</sub> O	1.03	0.45
TiO <sub>2</sub>	0.63	–
P <sub>2</sub> O <sub>5</sub>	0.64	–
LOI*	21.23	–

\* L.O.I: loss on ignition.

Fig. 4 displays SEM images of FS natural clay and Fau Y zeolite. Micrographics show an overall homogeneity of texture and regular shapes with high particle densification.

On one hand, FS natural clay presents a regular porous structure (see Fig. 4-A1 and 4-A2), without the presence of cracks or holes. However, some quartz grains are presented (≤10 μm). Inter-particle/agglomerate void spaces are also displayed that could contribute to natural clay porosity. On the other hand, in the Fau Y zeolite image (see Fig. 4-B1 and 4-B2) crystal shapes can be visualised. Coarse particles are also observed in Fau Y zeolite, with

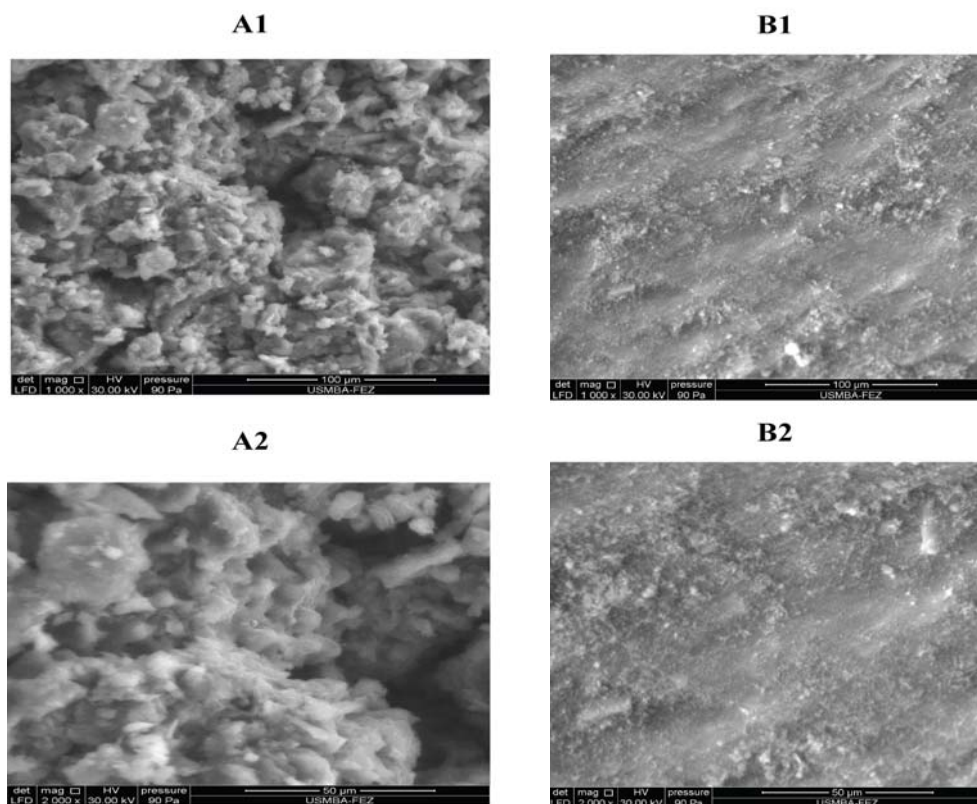


**Figure 4.** SEM pictures of the FS natural clay (A1-A2) and Fau Y zeolite (B1-B2).

the presence of void spaces that could contribute to the porosity of Fau Y zeolite.

Fig. 5 illustrates the results of thermogravimetric analyses (TGA) conducted on FS natural clay sample. TG curve shows the change in sample weight, and DTG curve displays derivative weight loss, as a function of temperature. FS sample has a total weight loss about 21.24% between 373 and 1273 K. The first registered weight loss (until 273 K) corresponds to the desorption of

undissociated water. The second loss of weight occurs at 852K and could correspond to water removal from the clay mineral composition.<sup>40</sup> The weight loss that takes place at 1136 K could be related to calcite  $\text{CaCO}_3$  decomposition.<sup>41</sup>

Infrared spectrum of FS natural clay is shown in Fig. 6 and indicates the presence of absorption bands corresponding to Si–O, Al–O, Mg–O, Fe–O and Ca–O vibrations (3622, 3399, 1635, 1421, 996, 872, 727, 530, and

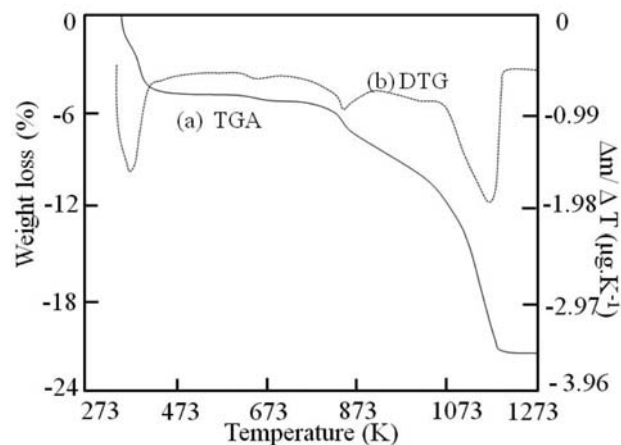


**Figure 5.** Thermogravimetric analysis (TGA) of FS natural clay

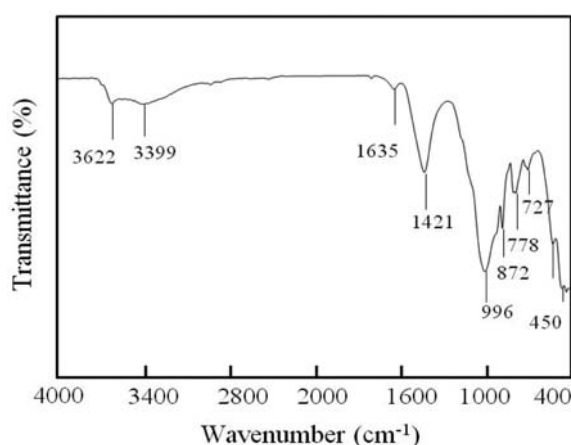


**Figure 6.** Infrared spectra of FS natural clay

450  $\text{cm}^{-1}$ , respectively). The presence of calcium could be associated with carbonates species (stretching bands near 1421 and 872  $\text{cm}^{-1}$ )<sup>42,43</sup> which are apparently related with the existence of calcite, in agreement with those results obtained by XRD and thermogravimetric analysis. Stretching vibrations of the surface hydroxyl groups (Si–Si–OH, or Al–Al–OH coupled by AlMgOH) are found at 3622  $\text{cm}^{-1}$ . Vibrations at 1635  $\text{cm}^{-1}$  is attributable to the bending of adsorbed water between the layers. Moreover, absorption bands at 996, 530 and 450  $\text{cm}^{-1}$  could arise due to stretching and bending vibrations of  $\text{SiO}_4^{2-}$  tetrahedral.<sup>44</sup> In the low frequency range (1200–650  $\text{cm}^{-1}$ ), maximum absorption of silicate minerals was observed at 996  $\text{cm}^{-1}$  while bands at 530 and 450  $\text{cm}^{-1}$  could be to Al–O–Si and Si–O–Si bending vibrations, respectively.

### 3. 2. Adsorption Capacities of FS Natural Clay and Fau Y Zeolite Towards VOCs

Fig. 7 displays adsorption equilibrium data of selected VOCs (benzaldehyde, methanol, and toluene) at 300 K onto FS natural clay and Fau Y zeolite samples, after the outgassing step at 383 K for 24 h. Adsorption equilibrium data are reported as mol of adsorbed VOC per mass of solid ( $\text{mol}_{\text{adsorbed VOC}} \text{g}_{\text{solid}}^{-1}$ ). Experimental adsorption data fit to Langmuir adsorption isotherm model very well.<sup>45</sup>

$$q_e = \frac{K C_{\text{VOC}} q_m}{(1 + K C_{\text{VOC}})} \quad (2)$$

where  $q_e$  is the amount of adsorbed VOC (benzaldehyde, methanol, or toluene) on the natural clay FS or Fau Y zeolite at equilibrium [ $\text{mol g}^{-1}$ ],  $C_{\text{VOC}}$  is the concentration of

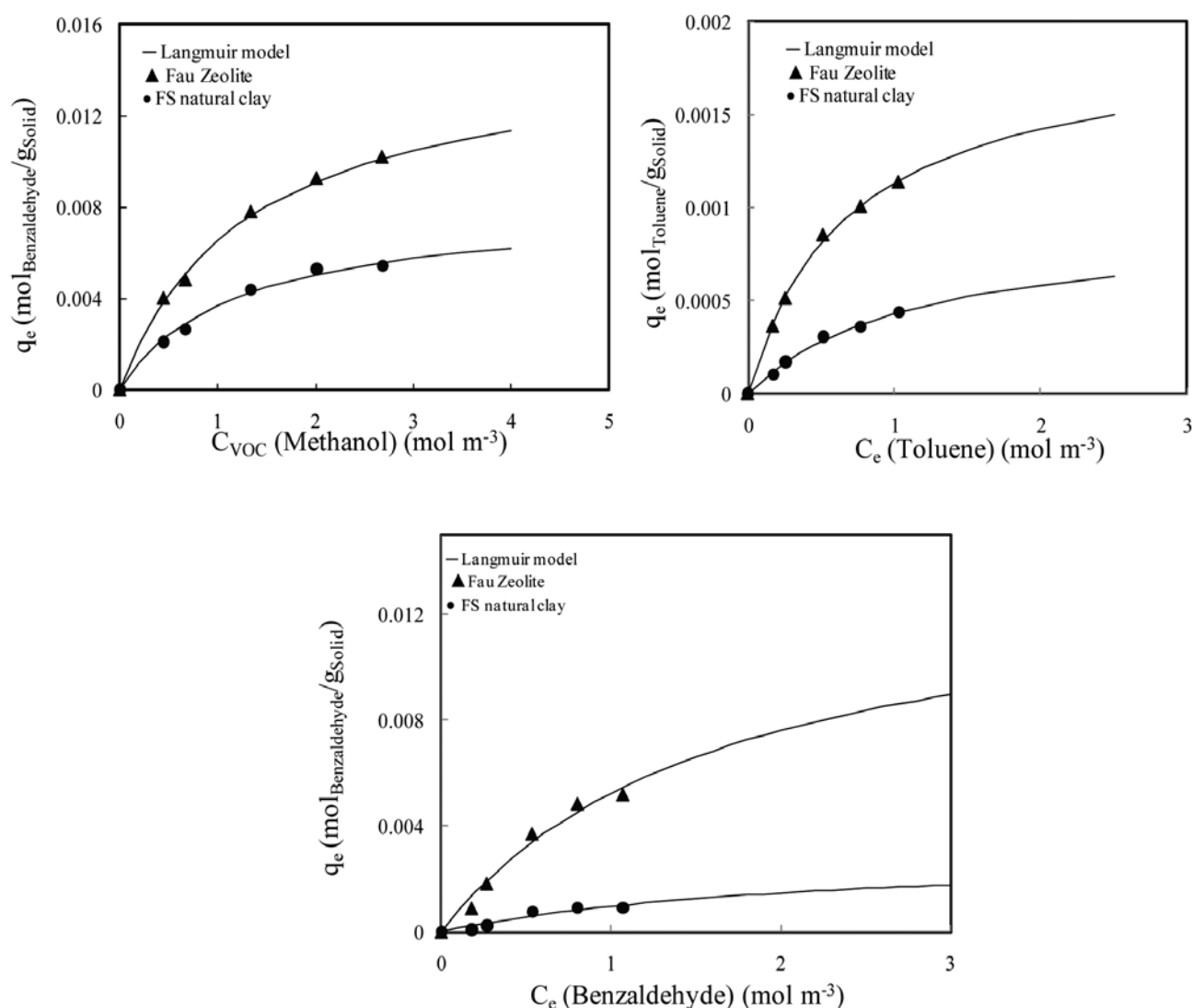


**Figure 7.** Comparison of adsorption capacities toward different VOCs (benzaldehyde, methanol, and toluene) of (▲) FS natural clay and (●) Fau Y zeolite, (–) represents the fit to Langmuir adsorption model.

the selected VOC (benzaldehyde, methanol, or toluene) at the equilibrium ( $\text{mol m}^{-3}$ ),  $q_m$  is the maximum adsorption capacity [ $\text{mol g}^{-1}$ ], and  $K$  is the adsorption equilibrium constant or Langmuir constant [ $\text{m}^3 \text{mol}^{-1}$ ]. Langmuir sorption model has been applied to VOC adsorption on synthetic zeolites.<sup>37,46</sup>

The maximum adsorption capacity,  $q_m$ , and the adsorption equilibrium constant,  $K$ , are determined from the intercept and the slope of the linearised form of Langmuir plot. The values of different parameters of the Langmuir adsorption model at 300 K together with the correlation factor,  $R^2$ , for the selected VOC on natural clay and Faujasite Y zeolite samples are summarised in Table 4. Additio-

nally, the maximum adsorption capacity is also expressed in  $\text{mmol m}^{-2}$ , corresponding to monolayer coverage and it is here defined as  $S_r$ .

As it can be seen in Fig. 7 and as expected, the adsorption capacities of FS natural clay and Fau Y zeolite, increase as the concentration of VOCs increases.<sup>44</sup>

Results indicate that FS natural clay has lower uptake capacity toward all VOCs assessed here. The greatest adsorption capacity of Fau Y zeolite could be due to its large specific surface area ( $S_{\text{BET}}$ ) and total pore volume.

Results listed in Table 4 shows that FS natural clay has higher adsorption affinity toward aliphatic hydrocarbons (methanol  $8 \text{ mmol g}^{-1}$ ) than for aromatic compounds

**Table 4.** Adsorption equilibrium constants of adsorbed VOCs onto FS natural clay and Fau Y zeolite obtained by the Langmuir adsorption model at 300K.

VOCs	Sample	Langmuir			$R^2$
		$q_m$ [ $\text{mmol g}^{-1}$ ]	$S_r$ [ $\text{mmol m}^{-2}$ ]	$K$ [ $\text{m}^3 \text{mol}^{-1}$ ]	
Methanol	FS natural clay	8	0.276	0.852	0.99
	Fau Y zeolite	15	0.027	0.811	0.98
Toluene	FS natural clay	0.89	0.031	0.889	0.98
	Fau Y zeolite	1.91	0.003	1.456	0.97
Benzaldehyde	FS natural clay	3.1	0.107	0.450	0.97
	Fau Y zeolite	13.9	0.025	0.604	0.95

**Table 5.** Comparison of adsorption capacities toward benzaldehyde (B), methanol (M), or toluene (T) of FS natural clay and some other adsorbents reported in the literature.

Adsorbent	VOCs	Temperature (K)	Adsorption capacity ( $\text{mmol/g}$ )	References
FS natural clay	T	300	0.89	Present work
Fau Y	T	300	1.99	Present work
ZSM-5	T	300	0.93	46
MS13X	T	300	3.7	49
MOF-177	T	298	6.35	20
NaY	T	300	1.36	56
ZnY	T	300	1.25	
NiY	T	300	3.59	
AgY	T	300	3.65	
ZSM-5 sorbents	T	299	1.55–1.57	57
HMOR	T	298	2–3	49
Raw clay	T	298	0.016	34
DDMA–clay	T	298	0.02	34
porous clay heterostructures (PCH)	T	298	1.53	35
FS natural clay	M	300	8	Present work
SAPO-34	M	300	15	58
ZSM-5 sorbents (HZSM or NaZSM-5/180)	M	299	0.83–1.1	57
Faujasite $\text{StY}_2\text{-L}$	M	299	2.21	57
Faujasite $\text{SiCl}_4\text{Y}_2\text{-L}$	M	299	1.57	57
HMOR	M	299	3.08	57
MCM-41	M	299	11–21	59
Zeolite (HY901, MS13X)	M	298	10–12	49
Activated carbon	B	303	0.79	60

(toluene  $0.91 \text{ mmol g}^{-1}$ ). These results could be attributed to the pore size of the FS natural clay in relation to the kinetic diameters of the VOCs ( $4 \text{ \AA}$  for methanol and  $5.8 \text{ \AA}$  for toluene).

Maximum adsorption capacities of FS natural clay,  $q_m$ , at 300 K led to the following adsorption order: methanol ( $8 \text{ mmol g}^{-1}$ ) > benzaldehyde ( $3.1 \text{ mmol g}^{-1}$ ) > toluene ( $0.89 \text{ mmol g}^{-1}$ ). Fau Y zeolite shows the highest affinity toward methanol adsorption ( $15 \text{ mmol g}^{-1}$ ) followed by benzaldehyde ( $13.9 \text{ mmol g}^{-1}$ ) and toluene ( $1.91 \text{ mmol g}^{-1}$ ). These results are in agreement with those obtained by SEM analysis where Fau Y zeolite shows a higher developed microporous structure, than FS natural clay (see Fig. 4).

Non-aromatic molecule such as methanol with small kinetic diameter<sup>16</sup> around  $4 \text{ \AA}$  can be easily adsorbed into the FS natural clay; whereas aromatic molecules (toluene and benzaldehyde) with relatively larger kinetic diameters in the range of  $5.8\text{--}6.8 \text{ \AA}$  have difficulty being adsorbed due to their larger sizes.<sup>47–49</sup> For Fau Y zeolite, with a mesoporous structure, largest molecules (benzaldehyde and toluene) can easily be adsorbed.<sup>50,51</sup> In addition, Si/Al ratio is another important parameter that affects adsorption capacity of adsorbents.<sup>52,53</sup> Fau Y zeolite has higher Si/Al ratio than FS natural clay. This parameter may also explain the higher adsorption capacity of Fau Y zeolite as compared to FS natural clay. Munthali et al.<sup>54</sup> has reported that zeolites with higher negative charge density had greater selectivity for  $\text{H}^+$ . On the other hand, the degree of hydrophobicity is normally dependent on the Si/Al ratio.<sup>55</sup> Fau Y zeolite with high specific surface area ( $S_{\text{BET}}$ ) making zeolite as an-effective sorbent for pollution control purposes, especially for the removal of VOCs from waste gas streams.

As a way of comparison, Table 5 lists the amount of adsorbed VOCs (benzaldehyde, methanol, or toluene) at the equilibrium onto FS natural clay (present work) and from literature references using different adsorbents under similar conditions. As it can be seen, adsorption capacities of natural clay toward benzaldehyde, methanol, and toluene are of the same order of those observed values using other porous adsorbents such as zeolites.

For possible industrial use of clay in the elimination of VOCs into the air, future work will focus on adsorption experiments in dynamical mode must be carried out similar to the work of Likoazar. et al and Zaitan et al.<sup>61–62; 32</sup>

### 3. 3. Effect of Temperature

As a way of illustration, Fig. 8 shows the effect of temperature on the adsorption of toluene onto FS natural clay. As it can be seen the adsorption capacity of FS natural clay toward toluene progressively decreases when temperature raises from 300 to 323 K. At a concentration of toluene of  $0.51 \text{ mol m}^{-3}$ , toluene adsorption is reduced around a 40% with the increase on temperature from 300

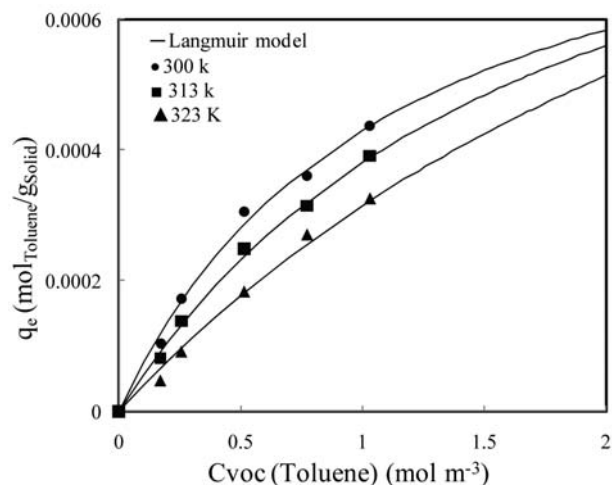


Figure 8. Effect of temperature on the adsorption capacity of FS natural clay toward toluene.

to 323 K, suggesting that the adsorption of VOCs onto FS natural clay is an exothermic process. Similarly, Moghadam et al.<sup>56</sup> have observed that toluene adsorption onto *Glycyrrhiza glabra* root is reduced with the increase of temperature.

Adsorption enthalpy is estimated using Van't Hoff method, relating the changes in the adsorption equilibrium constant,  $K$ , with the change in temperature,  $T$ , as described by equation (3):

$$\ln K = -\left(\frac{\Delta H}{RT}\right) + \left(\frac{\Delta S}{R}\right) \quad (3)$$

where  $\Delta H$  is the adsorption enthalpy ( $\text{kJ mol}^{-1}$ ),  $\Delta S$  is the entropy change ( $\text{kJ mol}^{-1}\text{K}^{-1}$ ),  $T$  is the absolute temperature (K) and  $R$  is the gas constant ( $0.008314 \text{ kJ mol}^{-1}\text{K}^{-1}$ ). Thus,  $\Delta H$  is estimated from the slope of the linear van't Hoff plot.

The obtained negative value of  $\Delta H$  ( $-54 \text{ kJ mol}^{-1}$ ) confirms the exothermic nature of toluene adsorption onto FS natural clay. Generally, physisorption has characteristic values between  $-20$  and  $-60 \text{ kJ mol}^{-1}$ ; whereas chemisorption has a range of  $-80$  to  $-400 \text{ kJ mol}^{-1}$ .<sup>63</sup> It should be noticed that the adsorption enthalpy value obtained here is 1.38 times the value of toluene evaporation heat ( $39.2 \text{ kJ mol}^{-1}$ ).<sup>64</sup> It could be concluded that toluene adsorption on FS clay is mainly a physical process. In fact, the low heat of adsorption may be considered as advantage in a procedure that includes a desorption/regeneration step of the adsorbent and VOC recovery.

### 3. 4. Analysis of Adsorbent Costs

In this section a preliminary analysis of operating cost related to the use of FS natural clay and Fau Y zeolite for the removal of VOCs is conducted. As it can be seen in



Table 4, the maximum adsorption capacity of Fau Y zeolite at 300 K, is almost 2 to 4 times higher than the values of FS natural clay. This means that FS natural clay in order to have an equivalent adsorption capacity to Fau Y zeolite, it is necessary to use a mass of FS natural clay 2–4.5 times higher than that required mass of Fau Y zeolite.

If it is considered an estimated average price of FS natural clay to be around US\$ 0.02 kg<sup>-1</sup>, it will yield an additional advantage in terms of operating cost, being 500 times lower than those values obtained when Fau Y zeolite is used (US\$ 10 kg<sup>-1</sup>). Nevertheless, comparing the cost per solid surface area (US\$/m<sup>2</sup>), values of 1.81 × 10<sup>-5</sup> and 6.9 × 10<sup>-7</sup> US\$/m<sup>2</sup> are obtained for Fau Y zeolite and FS clay, respectively; which is 26 times in favour of natural clay. Thus, given the fact of abundance and low cost, natural clay is likely to become a strong adsorbent candidate for VOC removal.

## 4 Conclusions

In this work clay natural was evaluated with regards to their possible use in removal of VOCs from waste gas. Adsorption capacity results of FS natural clay toward methanol, toluene and benzaldehyde as representatives VOCs suggest that FS natural clay could be applicable for controlling the emissions of VOCs. Although, commercial Fau Y zeolite shows a higher adsorption capacity for all the VOCs used in this study, FS natural clay is more abundant and its low acquisition cost makes it an efficient and economic natural adsorbent for the removal of VOCs from contaminated gaseous streams. Hence, natural clay used in this study has good possibilities to be applied as adsorbent of VOCs regarding its performances and lower cost.

## 5. Acknowledgements

Authors gratefully acknowledge the Centre National pour la Recherche Scientifique et Technique of Morocco (CNRST), the Centre national de la recherche scientifique of France (CNRS) with the Project (CNRST/CNRS No. SPI 05/13), Embassy of France in Egypt, French Institute in Cairo EGYPT, Comisión Nacional de Investigación Científica y Tecnológica of Chile (CONICYT) and Fondo Nacional de Desarrollo Científico y Tecnológico of Chile (FONDECYT) with the Project (CONICYT/FONDECYT Grant No. 1130560), for their financial support.

## 6. References

1. F. Khan, A. Ghoshal, *J. Loss. Prev. Proc. Ind.* **2000**, *13*(6), 527–545.  
[http://dx.doi.org/10.1016/S0950-4230\(00\)00007-3](http://dx.doi.org/10.1016/S0950-4230(00)00007-3)
2. T. Ohura, T. Amagai, X. Y. Shen, S. Li, P. Zhang, L. Z. Zhu,

- Atmos. Environ.* **2009**, *43*, 6352–6359.  
<http://dx.doi.org/10.1016/j.atmosenv.2009.09.022>
3. B. Guieysse, C. Hort, V. Platel, R. Munoz, M. Ondarts, S. Revah, *Biotechnol. Adv.* **2008**, *26*, 398–410.  
<http://dx.doi.org/10.1016/j.biotechadv.2008.03.005>
4. H. Wang, L. Nie, J. Li, Y. Wang, G. Wang, J. Wang, Z. Hao, *Chin. Sci. Bull.* **2013**, *58*(7), 724730.  
<http://dx.doi.org/10.1007/s11434-012-5345-2>
5. A. J. Cohen, *Environ. Health. Perspect.* **2000**, *108*, 743–750.
6. United States Environmental Protection Agency (USEPA), Volatile Organic Compounds Emissions,  
<https://cfpub.epa.gov/roe/indicator.cfm?i=23#3>, **2014**.
7. EEA Technical report, Annual European Community LRTAP Convention emission inventory report 1990–2006 Submission to EMEP through the Executive Secretary of the UNECE. EEA Technical report. No 7/2008. ISBN 978-92-9167-366-7.
8. M. L. Rodríguez, L. E. Cadús, D. O. Borio, *Chem. Eng. J.* **2016**, *306*, 86–98.  
<http://dx.doi.org/10.1016/j.cej.2016.05.055>
9. M. Kampa, E. Castanas, *Environ. Pollut.* **2008**, *151*, 362–367.  
<http://dx.doi.org/10.1016/j.envpol.2007.06.012>
10. I. Faisal, V. K. Khan, *J. Loss. Prev. Process. Ind.* **2000**, *13*, 527–545.  
[http://dx.doi.org/10.1016/S0950-4230\(00\)00007-3](http://dx.doi.org/10.1016/S0950-4230(00)00007-3)
11. V. R. Choudhary, K. Mantri, *Langmuir*, **2000**, *16*(17), 7031–7037. <http://dx.doi.org/10.1021/la991714u>
12. A. K. Boulamanti, C. A. Korologos, C. J. Philippopoulos, *Atmos. Environ.* **2008**, *42*, 7844–7850.  
<http://dx.doi.org/10.1016/j.atmosenv.2008.07.016>
13. P. Monneyron, M-H. Manero, J. S. Pic, *Can. J. Chem. Eng.* **2007**, *85*, 326–332.  
<http://dx.doi.org/10.1002/cjce.5450850307>
14. E. N. Ruddy, L. A. Carroll, *Chem. Eng. Prog.* **1993**, *89*(7), 28–35.
15. A. K. Ghoshal, S. D. Manjare, *J. Loss. Prev. Process. Ind.* **2002**, *15*(6), 413–421.  
[http://dx.doi.org/10.1016/S0950-4230\(02\)00042-6](http://dx.doi.org/10.1016/S0950-4230(02)00042-6)
16. H. Zaitan, H. Valdés, Removal of volatile organic compounds (VOCs) using adsorption Process onto Natural Clays, in: K. Chetehouna, Volatile Organic Compounds: Emission, Pollution and Control, New York: Nova Publishers, **2014**, p. 169–207.
17. V. K. Gupta, N. Verma, *Chem. Eng. Sci.* **2002**, *57*, 2679–2696. [http://dx.doi.org/10.1016/S0009-2509\(02\)00158-6](http://dx.doi.org/10.1016/S0009-2509(02)00158-6)
18. X. Li, Z. Li, L. Luo, *Chin. J. Chem. Eng.* **2008**, *16*(2), 203–208. [http://dx.doi.org/10.1016/S1004-9541\(08\)60063-4](http://dx.doi.org/10.1016/S1004-9541(08)60063-4)
19. J. Pires, A. Carvalho, M. B. Carvalho, *Microporous Mesoporous Mater.* **2001**, *43*, 277–287.  
[http://dx.doi.org/10.1016/S1387-1811\(01\)00207-4](http://dx.doi.org/10.1016/S1387-1811(01)00207-4)
20. L. Chu, S. Deng, R. Zhao, Z. Zhang, C. Li, X. Kang, *RSC Adv.* **2015**, *5*, 102625–102632.  
<http://dx.doi.org/10.1039/C5RA22597C>
21. T. El Brihi, J. N. Jaubert, D. Barth, L. Perrin, *Environ. Technol.* **2003**, *24*(10), 1201–1210.  
<http://dx.doi.org/10.1080/09593330309385662>

22. P. Le Cloirec, *Chin. J. Chem. Eng.* **2012**, *20*, 461–468.  
[http://dx.doi.org/10.1016/S1004-9541\(11\)60207-3](http://dx.doi.org/10.1016/S1004-9541(11)60207-3)
23. H. F. Cheng, M. Reinhard, *Environ. Sci. Technol.* **2006**, *40*, 7694–7701. <http://dx.doi.org/10.1021/es060886s>
24. X. Zhao, Q. Ma, G. Q. Max Lu, *Energy Fuels* **1998**, *12*, 1051–1054. <http://dx.doi.org/10.1021/ef980113s>
25. X. Tao, T. Yang, T. Chang, T. Chung, *J. Environ. Eng.* **2004**, *130*, 1210–1216.  
[http://dx.doi.org/10.1061/\(ASCE\)0733-9372\(2004\)130:10\(1210\)\)](http://dx.doi.org/10.1061/(ASCE)0733-9372(2004)130:10(1210)))
26. M. W. Ackley, S. U. Rege, H. Saxena, *Microporous Mesoporous Mater.* **2003**, *61*, 25–42.  
[http://dx.doi.org/10.1016/S1387-1811\(03\)00353-6](http://dx.doi.org/10.1016/S1387-1811(03)00353-6)
27. C. Julcour, C. Andriantsiferana, N. Krou, C. Ayral, E. Mohamed, A. Wilhelm, H. Delmas, L. Le Coq, C. Gerente, K. M. Smith, S. Pullket, G. D. Fowler, N. J. Graham, *J. Environ. Manag.* **2010**, *91*(12), 2432–2439.  
<http://dx.doi.org/10.1016/j.jenvman.2010.06.008>
28. J. F. Vivo-Vilches, A. F. Pérez-Cadenas, F. Carrasco-Marín, F. J. Maldonado-Hódá, *J. Environ. Chem. Eng.* **2015**, *3*, 2662–2669.  
<http://dx.doi.org/10.1016/j.jece.2015.09.027>
29. M. Eloussaief, A. Sdiri, M. Benzina, *Environ. Sci. Pollut. Res.* **2013**, *20* (1), 469–479.  
<http://dx.doi.org/10.1007/s11356-012-0874-4>
30. M. Mhamdi, H. Galai, N. Mnasri, E. Elaloui, M. Trabelsi-Ayadi, *Environ. Sci. Pollut. Res.* **2013**, *20* (3), 1686–1697.  
<http://dx.doi.org/10.1007/s11356-012-1015-9>
31. H. Zaitan, T. Chafik, T. C. R. *Chimie* **2005**, *8* (9–10), 1701–1708. <http://dx.doi.org/10.1016/j.crci.2005.05.002>
32. H. Zaitan, D. Bianchi, O. Achak, T. Chafik, *J. Hazard. Mater.* **2008**, *153*, 852–859.  
<http://dx.doi.org/10.1016/j.jhazmat.2007.09.070>
33. N. Dammak, N. Fakhfakh, S. Fourmentin, M. Benzina, *J. Environ. Chem. Eng.* **2013**, *1*, 667–675.  
<http://dx.doi.org/10.1016/j.jece.2013.07.001>
34. I. Jarraya, S. Fourmentin, M. Benzina, S. Bouaziz, *Chem. Geology*, **2010**, *275*, 1–8.  
<http://dx.doi.org/10.1016/j.chemgeo.2010.04.004>
35. F. Qu, L. Zhu, K. Yang, *J. Hazard. Mater.* **2009**, *170*, 7–12.  
<http://dx.doi.org/10.1016/j.jhazmat.2009.05.027>
36. S. Bertrand, F. Charlet, E. Chapron, N. Fagel, M. Batist, *Palaeogeogr. Palaeoclimatol. Palaeoecol.* **2008**, *259*, 301–322.  
<http://dx.doi.org/10.1016/j.palaeo.2007.10.013>
37. S. Brosillon, M. H. Manero, J. Foussard, *Environ. Sci. Technol.* **2001**, *35*, 3571–3575.  
<http://dx.doi.org/10.1021/es010017x>
38. A. Atterberg, Die Plastizität der Tone., Internationale Mitteilungen für Bodenkunde, **1911**, *1*, 10–43.
39. F. A. Andrade, H. A. Al-Qureshi, D. Hotza, *Appl. Clay. Sci.* **2011**, *51*, 1–7.  
<http://dx.doi.org/10.1016/j.clay.2010.10.028>
40. F. Ayari, E. Srasra, M. Trabelsi-Ayadi, *Desalination* **2005**, *185*, 391–397.  
<http://dx.doi.org/10.1016/j.desal.2005.04.046>
41. M. V. Kök, *Energy Sources* **2002**, *24*(10), 899–907.  
<http://dx.doi.org/10.1080/00908310290086833>
42. N. V. Vagenas, A. Gatsouli, C. G. Kontoyannis, *Talanta* **2003**, *59*, 831–836.  
[http://dx.doi.org/10.1016/S0039-9140\(02\)00638-0](http://dx.doi.org/10.1016/S0039-9140(02)00638-0)
43. A. Sdiri, T. Higashi, T. Hatta, F. Jamoussi, N. Tase, *Environ. Earth. Sci.* **2010**, *61*(6), 1275–1287.  
<http://dx.doi.org/10.1007/s12665-010-0450-5>
44. V. C. Farmer, The layer silicates, in: V.C. Farmer (Ed.), *The Infrared Spectra of Minerals*, Mineralogical Society, London, **1974**.
45. I. Langmuir, *J. Am. Chem. Soc.*, **1918**, *40*(9), 1361–1403.  
<http://dx.doi.org/10.1021/ja02242a004>
46. H. Zaitan, M. H. Manero, H. Valdés, *J. Environ. Sci.* **2016**, *41*, 59–68  
<http://dx.doi.org/10.1016/j.jes.2015.05.021>
47. E.G. Derouane, *Stud. Surf. Sci. Catal.*, **1980**, *5*, 5–18.  
[http://dx.doi.org/10.1016/S0167-2991\(08\)64860-0](http://dx.doi.org/10.1016/S0167-2991(08)64860-0)
48. Y. H. Ma, T. D. Tang, L. B. Sand, L. Y. Hou, *Stud. Surf. Sci. Catal.* **1986**, *28*, 531–538.  
[http://dx.doi.org/10.1016/S0167-2991\(09\)60916-2](http://dx.doi.org/10.1016/S0167-2991(09)60916-2)
49. K. J. Kim, H. G. Ahn, *Microporous Mesoporous Mater.* **2012**, *152*, 78–83.  
<http://dx.doi.org/10.1016/j.micromeso.2011.11.051>
50. K. Chae, Y. Siberio-Pérez, J. Kim, Y. Go, M. Eddaoudi, J. Matzger, M. O’Keeffe, M. Yaghi, *Nature*, **2003**, *427*, 523–527. <http://dx.doi.org/10.1038/nature02311>
51. F. Qian, B. Li, Y. Hu, G. Niu, Y. Zhang, C. Renchao, T. Yi, D. Su, A. Asiri, D. Zhao, *Chem-A Eur. J.* **2012**, *18*, 931–939.  
<http://dx.doi.org/10.1002/chem.201102505>
52. P. Harben, *The industrial minerals handybook*. 4<sup>th</sup> ed., Industrial minerals information 11 Ltd., London, **2002**
53. A. M. Ziyath, P. Mahbub, A. Goonetilleke, M. O. Adebajo, S. Kokot, A. Oloyede, *J. Water Resource Prot.* **2011**, *3*, 758–767. <http://dx.doi.org/10.4236/jwarp.2011.310086>
54. M. Munthali, M. Elsheikh, E. Johan, N. Matsue, *Molecules*, **2014**, *19*, 20468–20481.  
<http://dx.doi.org/10.3390/molecules191220468>
55. M. Oliveira, A. Miranda, C. Barbosa, C. Cavalcante, D. Azevedo, E. Castellon, *Fuel*, **2009**, *88*, 1885–1892.  
<http://dx.doi.org/10.1016/j.fuel.2009.04.011>
56. F. Mohammadi-Moghadam, M.M. Amin, M. Khiadani, F. Momenbeik, H. Nourmoradi, M.S. Hatamipour, *J. Environ. and Public Health*, **2013**, *2013*, 1–7.  
<http://dx.doi.org/10.1155/2013/986083>
57. C. K. W. Meininghaus, R. Prins, *Microporous and Mesoporous Mater.* **2000**, *35–36*, 349–365.  
[http://dx.doi.org/10.1016/S1387-1811\(99\)00233-4](http://dx.doi.org/10.1016/S1387-1811(99)00233-4)
58. Y. Kobayashi, Y. Li, Y. Wang, D. Wang, *Chin. J. Cat.* **2013**, *34*, 2192–2199.  
[http://dx.doi.org/10.1016/S1872-2067\(12\)60676-7](http://dx.doi.org/10.1016/S1872-2067(12)60676-7)
59. M. M. M. Ribeiro Carrott, A. J. E. Candeias, P. J. M. Carrott, P. I. Ravikovitch, A. V. Neimark, A. D. Sequeira, *Microporous and Mesoporous Mater.* **2001**, *47*, 323–337.  
[http://dx.doi.org/10.1016/S1387-1811\(01\)00394-8](http://dx.doi.org/10.1016/S1387-1811(01)00394-8)
60. R. K. Rajoriya, B. Prasad, I. M. Mishra, K. L. Wasewar, *Chem. Biochem. Eng. Q.* **2007**, *21*(3), 219–226.

61. B. Likozar, D. Senica, A. Pavko, *Ind. Eng. Chem. Res.* **2013**, 52, 9247–9258. <http://dx.doi.org/10.1021/ie400832p>
62. B. Likozar, D. Senica, A. Pavko, *Brazilian j. of chem. Eng.* **2012**, 29 (3), 635–652.
63. Y. Yu, Y. Zhuang, Z. H. Wang, *J. Colloid. Interface. Sci.* **2001**, 242(2), 288–293. <http://dx.doi.org/10.1006/jcis.2001.7780>
64. D. D. Do, *Adsorption Analysis: Equilibria and Kinetics*. London: Imperial College Press, **1998**.

## Povzetek

Številni problemi onesnaževanja okolja nastanejo zaradi emisije topnih organskih snovi (VOC) in posledično zato postaja njihova kontrola resen izziv za kemijsko industrijo. Zaradi nekaterih prednosti je adsorpcija pogosto uporabljena tehnika za odstranjevanje VOC. V predstavljenih raziskavah so bile z različnimi fizikalno kemijskimi metodami določene karakteristike lokalno dostopne glin kot adsorbenta in proučena adsorpcija toluena, metanola in benzaldehida. Adsorpcijske izoterme so bile dobljene pri sobni temperaturi, podatki pa obdelani z Langmuirjevim modelom, ki omogoča določitev maksimalne adsorpcijske kapacitete ( $q_m$ ). Dvig temperature od 300 K na 323 K zniža adsorpcijsko kapaciteto toluena na glini. Določena je bila tudi adsorpcijska entalpija toluena na glini, ki znaša  $-54 \text{ kJ mol}^{-1}$ . Primerjava z zeolitom Fau Y kot komercialnim adsorbentom kaže, da ima ta sicer višje adsorpcijske kapacitete, je pa zato precej dražji: cena za kilogram je 10 USD, za glino pa 0.02 USD. Tako lahko glina služi kot alternativni adsorbent z nizko ceno.